Presented at SPIE Conference on MOEMS and Miniaturized Systems, San Francisco, CA, Feb 1st, 2020

Comparison of MEMS Mirror LiDAR Architectures

Abhishek Kasturi, Veljko Milanović, Daniel Lovell, Frank Hu, Derek Ho, Yu Su, Lj. Ristic
Mirrorcle Technologies, Inc., Richmond, CA

ABSTRACT

LiDAR systems in applications such as autonomous mobile robots, drones, vehicles, and other commercial applications that demand compact, low-cost, and dynamic scanning will inevitably turn to MEMS mirrors as the beam-steering component. Beam scanning-based LiDAR architectures have a significant advantage as the full power and attention of the sensor is given sequentially to each point (voxel) in the scan. Competitive LiDAR designs typically utilize scanning and are differentiated by their scanning architecture and the specific hardware utilized, with the general goal of moving away from bulky mechanical and motor-based systems and toward compact silicon-based MEMS technology.

Both single-axis and dual-axis MEMS mirrors are employed to enable two-dimensional (2D LiDAR) and three-dimensional (3D LiDAR) point cloud sensing, respectively. The underlying time-of-flight sensor can be generic – a laser rangefinder or single-point LiDAR, with any typical wavelength or sensing method (pulsed ToF, AMCW, FMCW, etc.). The sensor is arranged with scanning elements which brings forth challenging trade-offs, discussed here. Architectures differ in whether transmitter and receiver are arranged coaxially or biaxially, each with its advantages and disadvantages. We present a hybrid architecture, Synchronized MEMS Pair LiDAR (SyMPL), which simplifies the coaxial design significantly and increases its efficiency by removing any beam splitting components or beam dumps. Multiple prototype LiDARs are compared and evaluated on the basis of SNR, scan speed, robustness to shock and vibration, eye safety, and resilience to mutual interference and echo signals. The work discusses the varying impacts on manufacturing and cost for applications demanding large volumes of LiDAR systems.

Keywords: LiDAR, Scanning LiDAR, LiDAR Architecture, MEMS Mirrors, Coaxial, Biaxial, Transmitter development.

Glossary:

LiDAR	Light Detection and Ranging (also LADAR, Lidar, LIDAR)
FoV	Field of View
FoR	Field of Regard (sometimes used interchangeably with FoV)
iFoR	instantaneous Field of Regard (also iFoV)
LRF	Laser rangefinder
SNR	Signal-to-noise ratio
ADAS	Advanced Driver-Assistance Systems
AMR	Autonomous Mobile Robots
SyMPL	Synchronized MEMS Pair LiDAR
LUT	Look Up Table
ToF	Time-of-flight (distance measurement based on time light travels to target and back to receiver)

1. INTRODUCTION

1.1 INDUSTRY AUTOMATION AND TRANSPORTATION REVOLUTION

Today we are witnessing enormous transformation in industrial production, trend often described as Industry 4.0 [1][2]. Smart factories and smart warehouses that rely on smart machines and robots are becoming a reality. Deployment of robots and automation bring many advantages such as space optimization, process optimization, efficiency improvement, and flexibility in handling changes in operations. Mobile robots in particular, often called autonomous mobile robots (AMR), offer advantages in managing variations in demand by easily scaling up and down capacity or configuring a change in the work-flow to accommodate customization in manufacturing process. To be efficient in executing their tasks

mobile robots, besides other things required from them, need know-how to act 'on-the-fly' and adjust their routes through warehouses or other industrial facilities to avoid unexpected obstacles or humans. To accomplish that they need capability of sensing the space around them, namely perception sensing. Similarly, we are also witnessing a revolution in transportation [3][4][5][6] whereby safety features are becoming essential part of modern vehicles performance. And again, many of the safety features in modern cars are based on the capability of perception sensing [6].

1.2 TECHNOLOGIES FOR PERCEPTION SENSING

There are several competing technologies used for perception sensing around mobile robots or for safety ADAS applications in cars. These technologies include cameras, RADAR, LiDAR, and ultrasonic sensors [7][8][9]. Each one of these has advantages and disadvantages. Cameras offer wide angle and they are very good in interpreting signs and frontal shapes, but they lack depth and distance measurement capabilities. Simultaneous use of multiple cameras or stereo cameras may overcome disadvantages of using a single camera, but that type of solution requires extensive computation and it is slower than RADAR and LiDAR. LiDAR measures distance and creates a 3-D image of the surroundings. It is precise and also capable of detecting small objects, but these systems are still rather expensive, and a cloudy weather may adversely impact their performance. RADAR is mature obstacle detection technology, and cost effective given its maturity. It is capable of long-distance detection and less susceptible to weather conditions. But it also has limitations such as not being capable of producing precise object image nor detecting small objects. Ultrasonic sensors are typically used for detecting objects in a limited vicinity, up to 5 m. They are susceptible to adverse weather conditions such as heavy dust, rain, or snow and they can be used only at low speeds [10]. A disadvantage of these sensors is a lack of capability to detect small objects, but they are cost effective and already in wide use in cars for parking assistance. It is expected that all three technologies will co-exist and complement each other for some time.

However, when it comes to mid-range sensing (up to 30 m) it appears that MEMS LiDAR solution is becoming a leading contender. Compared to other solutions it shows clear advantage in performance including low average power, distance resolution in sub-cm range, object detection of varied materials and reflectance, fast scanning with programmable capability, and yet all of that accomplished at marketable price. Such a superior performance leads naturally to applications in mobile robots as well as in safety ADAS applications such as parking assistance, blind spot intervention, and lateral warning.

It should be pointed out that MEMS LiDAR solution relies on scanning the environment by using MEMS mirrors as essential part of system to produce 'cloud point' - a set of points presented in a 3-D coordinate system – in essence a 3-D picture of the surrounding environment around the robot or the car. This is commonly called perception sensing. The scanning performance of MEMS mirror is robust, with virtually limitless life-time since it is made of silicon crystal, it is small and compact device, and basically the only reliable scanning device suitable for mid-range LiDAR solutions.

1.3 MEMS MIRROR – ENABLER OF LIDAR SOLUTIONS

In the mid-2000s, a number of defense-related optical systems developers began to pursue new ways to reduce size, weight, power, and cost (or "SWaP-C") of optical sensors. New technologies were demanded by the Department of Defense branches and laboratories such as the Army Research Laboratory (ARL) as well as by related defense contractors. LiDAR systems for various small robotic platform DoD applications were being re-designed with the goal of major reduction in "SWaP-C". At that same time, in 2005 Mirrorcle Technologies entered the scene with Gimbal-less Two-Axis MEMS Mirrors which broke all the previous figure of merit barriers (for combined mirror size, tip-tilt angle, and speed). Replacement of galvanometer scanners in SWaP-C sensitive applications was no longer an academic discussion but a new commercial reality. Soon, the connection between the new generation LiDAR developers and MEMS mirrors became inevitable. By 2010, successful designs were deployed by Areté Associates, ARL, Spectrolab (Boeing), and a few years later by NGC Laser Systems and NASA Goddard Space Flight Center (GSFC). Those pioneering projects were enabled by the agile gimbal-less dual axis MEMS Mirrors. Just as importantly, further MEMS mirror developments strongly benefited from the demands and pressures of those projects, which were always commanding increases in the total figure of merit. By the mid-2010s, these MEMS mirrors enabled a whole genre of startups and developments of solid-state LiDAR technology proposed for autonomous driving applications and robotics.

Despite the numerous successful implementations of LiDAR solutions, including some commercial cases, there have been no suitable products available with the key features requested by the growing robotics industry - production readiness and marketable cost. Thus, the industry continues to heavily rely on solutions that are camera-based which cannot meet many of the requirements for robotic applications despite all the progress made in camera vision technology. This obviously points to an unmet demand for the mid-range, low cost, and low complexity LiDAR systems.

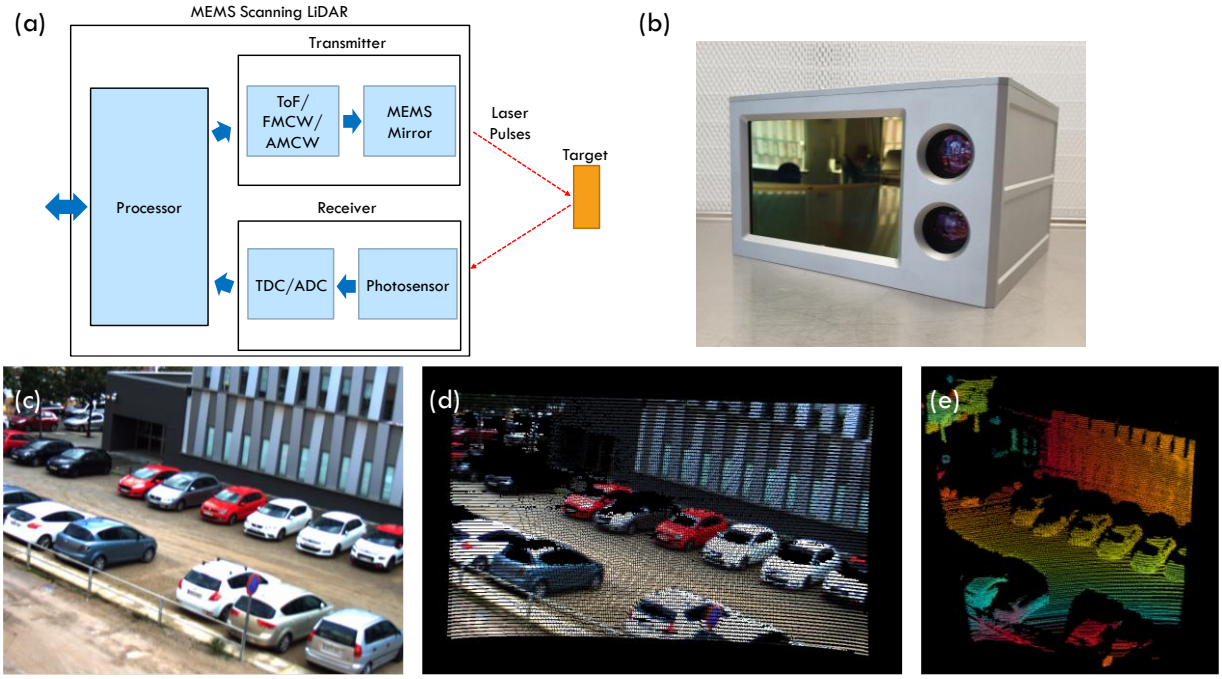

Figure 1. (a) A general system block diagram of a MEMS Scanning LiDAR (b) An example of a biaxial architecture 3D LiDAR system based on gimbal-less MEMS Mirrors, courtesy of Beamagine. (c) A scene imaged from a camera to compare alongside (d) an RGB fused image with the LiDAR scan, and (e) a pure point-cloud of the LiDAR scan, courtesy of Beamagine.

1.4 SCOPE OF THIS WORK

The scope of this review is a comparative analysis of different MEMS Mirror-based LiDAR Architectures and an investigation into distinctions in performance of various solutions. The analysis will focus on coaxial, biaxial, and hybrid architectures and will highlight fundamental advantages and disadvantages of each of the solutions. Since essential parts of every LiDAR solution are transmitter, receiver, scanning element, and controller different architectures will be described based on the arrangements of these elements. Also, discussion will include comments on basic performance parameters such as SNR, scan speed, robustness to shock and vibration, mutual interference performance as well as laser-safety performance.

2. MEMS MIRROR BASED LIDAR ARCHITECTURES

All scanning LiDARs fundamentally include a transmitter (radiation source), a receiver (detector), scanning component, and a controller which has the ability to control and co-ordinate the transmitter, receiver, and scanner in such a way that the system can provide measurements of distance of objects the radiation reflects from. This highly general composition naturally leads to a very large number of arrangements and measurement methodologies, and therefore a large number of architectures. In part this is due to the natural tendency of designers to seek novelty and intellectual property, but at the same time each application of a LiDAR system will have preferences for the inherent trade-offs of the different architectures. Here we review some more general aspects as they pertain to the use of MEMS Mirrors in beam steering for the LiDAR transmitter and/or receiver. Specifically, we will only focus on 3D LiDARs. That is, LiDARs which provide three-dimensional point clouds. For example, a point cloud that is based on the raster scan of 32 lines, with 120 measurement positions in each line, and a depth measurement at each position forms a 3-dimensional point cloud. We note that this can be accomplished by two-dimensional beam steering, but also with single-dimensional beam steering in arrangements where the transmitter and/or receiver are multi-channeled or multi-layered.

There are two main-architectures for MEMS mirror-based LiDAR systems – coaxial and biaxial. Coaxial LiDARs scan the outgoing laser beam and receive the reflected light back to the sensor using the same MEMS mirror while biaxial LiDARs place the sensor in an offset position from the transmitter and scanning components.

2.1 COAXIAL OR MONOSTATIC LIDAR WITH MEMS MIRRORS

In the coaxial arrangement, the transmitter and receiver components are arranged such that they are geometrically collocated and share the same FoV. Typically this FoV is very narrow, in fact often as narrow as the optical design allows, to allow precise pointing of the transmitter and receiver toward a specific target in the distance to obtain its distance information (see Fig. 3a). The beam-steering component is then placed in a position that allows it to direct this narrow transmitted beam and the narrow receiver's FoV together. The result is that the LRF now points to a specific instantaneous field of view (iFoV) which is programmably scanned over a wider area of FoV. For example the 0.1° iFoV may be scanned in 40 lines with 40 points across each line of a larger, 20°x20° FoV. This characteristic of directing the receiver simultaneously with the transmitted beam is a significant factor in increasing the resilience to mutual interference with other LiDARs in the field as well as against any other undesired light sources (sunlight etc.). The architecture can have a very high SNR and performance with accurate and long distance ranging, providing that the receiver has a large enough aperture for significant returning light collection. However, a distinct disadvantage of this setup is the requirement of a large enough mirror to maximize the amount of reflected light captured. Namely, if we take a typical LRF which can indeed range beyond 100m and quite accurately (Fig. 3a), and attempt to scan its transmitter and receiver, we may need to have a scanning mirror of 3-5cm diameter. Thus, coaxial architectures which attempt to utilize all of the advantages of MEMS mirror based scanning must take a significant trade-off with SNR as the receiving aperture must be significantly smaller than in typical LRFs.

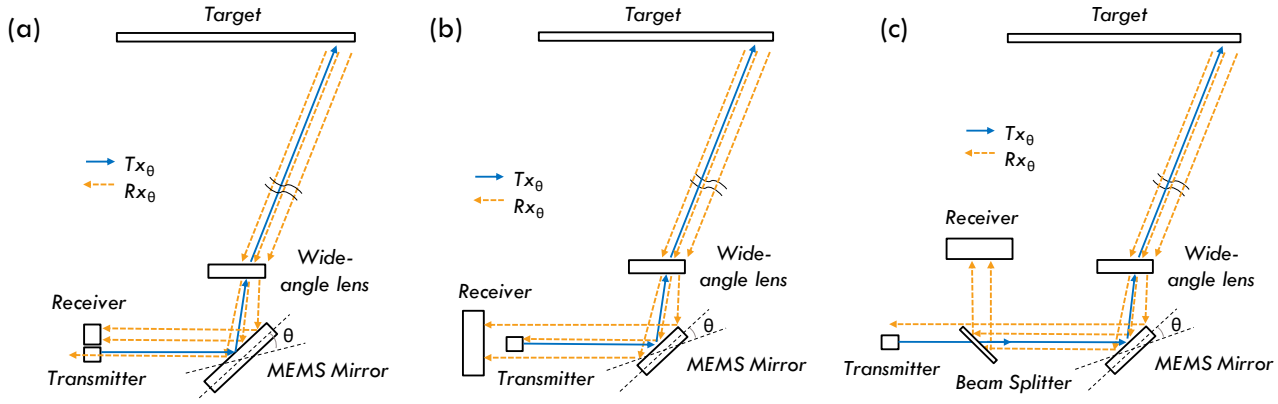

Figure 2. (a) The coaxial adjacent architecture places the receiver side-by-side with the transmitter and relies on an especially large MEMS Mirror (b) The coaxial concentric architecture places the receiver behind the transmitter. (c) The coaxial splitter architecture uses a beam splitter to minimize signal loss and the required MEMS Mirror size.

There are several methods of using a scanning mirror to transmit and receive the time of flight signal. Figure 2 shows three such methods, with each one in progression reducing the size of the scanning mirror to improve its speed and robustness and reduce its manufacturing cost. Figure 2a is the simplest arrangement, where any over the shelf (OTS) ToF transceiver solution (or LRF) where the transmitter and a small receiver are side by side. Such LRF setup is typically used with a large diameter mirror (e.g. >20mm) to scan the beam over the FoR and therefore is not actually useable with MEMS technology but instead must be a motorized or galvo solution. Figure 2b shows a way to reduce the mirror size to approach practical dimensions of MEMS mirrors (<10mm) and maintain some performance by overlapping the transmitter with the receiver, making it larger to accept more returned light, and using the optics to ensure the beam fits the MEMS mirror and the return light maximizes the use of the large receiver [11]. This would still require a relatively large MEMS mirror (e.g. >=10mm) to ensure enough SNR over the full distance range of 30m [37]. The key disadvantage of this setup of course is the loss of signal in the central portion of the returned light which the mirror deflects to the transmitter. Many conventional mechanical, spinning based LiDARs use this setup to perform 2D (X and Z) scanning systems. A nice example of this with a large motorized spinning mirror is the OLE Systems 2D LiDAR (LR-1B) in Fig. 3b.

The third method uses a beam splitter/combiner setup and is often used is biomedical imaging and similar systems – this is the most promising coaxial approach for MEMS mirrors in terms of reduced beam diameter and thus reduced mirror diameter requirement. In Richter et. al.'s work specifically using relatively small diameter MEMS mirrors (~2mm), a beam splitter is placed ahead of the transmitter, oriented at 45°, allowing the transmitted beam to pass through the splitter then reflect onto the receiver after returning from the target [13] (also in Fig. 3c). Figure 2c shows the optomechanical setup using a beam splitter to further reduce the MEMS mirror. In this setup, the beam splitter separates the path of the

transmitter and receiver, therefore requiring a more powerful pulsed laser source to generate the same amount of energy as the transmitters in Figure 2a and 2b. The key advantage in this setup would be a much smaller, faster and more robust MEMS mirror (<=5mm), being able to scan at fast rates or larger angles. The disadvantage is a more complex optical system requiring beam splitters and additional optics to maximize the light returned to the receiver [37].

The key design factor in all three cases of Figure 2 is the MEMS mirror size. The smaller the mirror diameter, the more practical the solution is in terms of the market demand – in terms of its mass manufacturability, its cost, its robustness against shock, qualification for automotive and industrial uses, and lower power consumption. Practical solutions can be achieved with reasonable trade-offs of performance and size with 5mm and 4.6mm diameter MEMS mirrors of the "bonded design" such as the A8L2.2-4600AU-TINY48.4. This is a 4.6mm diameter gold coated mirror, on an actuator with up to ±5.5° mechanical angle and a bandwidth of ~500Hz. Such a part could for example scan 500 lines per second (based on 250Hz period on the fast axis), providing a 12.5Hz 40-line scan, or a 20Hz 25-line raster scan. In other words the scan is fully programmable / arrangeable by system designer and can even be modified in real time by the system to achieve reconfigurable scanning LiDAR performance. The electrostatic MEMS actuator "A8L2.2" allows this dual-axis programmability, has excellent mechanical shock and vibration performance, less than a milliwatt power consumption, and is setup for standard silicon-based mass production.

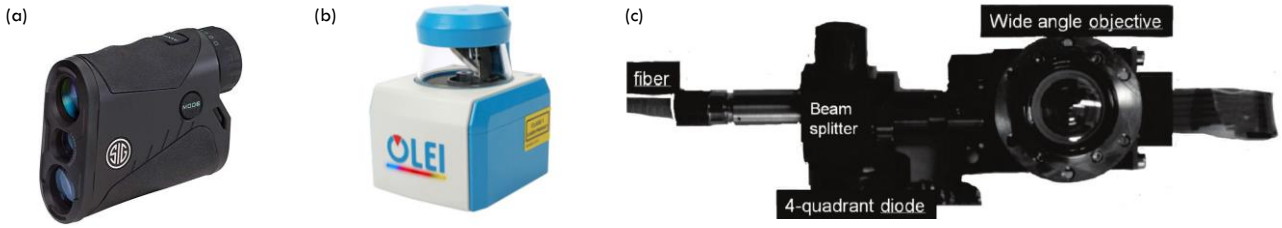

Figure 3. (a) An off-the-shelf point and range Laser Rangefinder that can be used in Figure 2a, (b) OLE systems spinning LiDAR (model LR-1B) implementing the coaxial concentric LiDAR architecture represented in Figure 2b (c) The coaxial splitter design by Richter, et. al. [13] as presented in Figure 2c.

Coaxial architectures often use NIR laser sources, most notably the OSRAM SPL90, 905nm pulsed laser, and sometimes 940nm sources. Since 905nm is within the responsivity of a Silicon based photodetector, low cost receivers can be used to build arrays of these systems. These components are relatively low cost compared to IR-Mid IR sources such as 1550nm or longer wavelengths, which require expensive InGaAs receivers. Nevertheless, all of those wavelengths are suitable for the 4.6mm and 5.0mm diameter and gold-coated mirror and have been successfully integrated into system designs.

2.2 BIAXIAL OR BISTATIC LIDAR WITH MEMS MIRRORS

In the biaxial architecture, the transmitter is paired with the MEMS mirror in a physically offset location from the receiver (Fig. 4). Park and Kim [15] describe an Independent Biaxial LiDAR using coded laser pulses, but fundamentally use the optomechanical architecture uses separate apertures for the transmitter and receiver. The biaxial approach (Figure 4a) was taken to give the transmitter side the flexibility of trying different scanning solutions to optimize the best FoV, angular resolution, frame rate and laser power handling [16]. Here, the iFoR is determined independently of the receiver, only by the transmitter design (wavelength, aperture size, angle magnification optics, laser divergence). And as the iFoR is scanned by the MEMS mirror over the overall FoR, the receiver must be able to receive and process returned light from any of those angles. Thus, this adds more strain on the receiver observing the entire FoV, or in some cases, portions of it, and receiving potentially stray light as well from various angles. Of course, the key benefit in this arrangement is that the receiver may be designed with "arbitrarily large" optics as it is not constrained by the scanning element. Receiver aperture (fiber taper, concentrator or another collection method) may be 25mm or larger as needed while the scanning element may be only 1-2mm diameter MEMS mirror. Additional transmitter encoding and receiver optical and electronic filtering may be needed to pick out the ToF pulses from own, preferred light pulses. Nonetheless, this setup is more optimal for use with MEMS mirrors since the transmitter can be separately designed without receive-light considerations and thus can use very fast, robust, and low cost small-diameter mirrors.

Figure 4c illustrates another approach presented by Koppal et. al [20]; it uses a simple ToF laser rangefinder setup and instead of using a large diameter mirror to steer the entire transceiver path, only the transmitter side is scanned to increase the FoR and make it programmable, and a stationary reflector and optics are used to observe the entire FoV. This receiver design drastically reduces the SNR and can be used in evaluation purposes to investigate the MEMS mirrors at shorter distances.

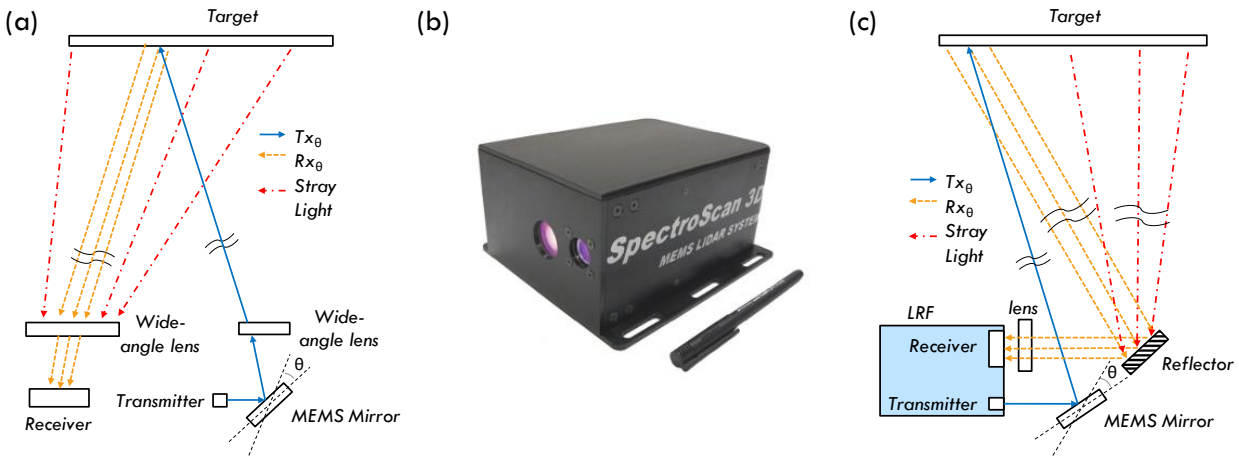

Figure 4. (a) Standard biaxial LiDAR design showing the receiver offset from the transmitter. (b) Boeing SpectroScan 3D, a commercialized biaxial MEMS Mirror LiDAR [17] (c) The biaxial design used by University of Florida researchers in [20]

Since the MEMS mirror is not part of the receiver's optical train and is not responsible for reflecting signals back towards the receiver, the biaxial architecture allows for the MEMS mirror's size to be smaller and therefore faster. The benefits of high-bandwidth MEMS mirrors are more than just increased scanning speeds; they also have a higher natural resonant frequency, making them more robust to shock and vibration. Since a smaller mirror can be used, biaxial architecture based LiDARs use a fiber coupled source, such as a 1550nm pulsed fiber laser. These mid-IR fiber sources can also have a higher pulse frequency, meaning larger sample rates resulting in higher resolutions if coupled with a fast scanning mirror. Typically, the integrated MEMS mirrors such as the A7M20.1-2000AL-TINY20.4 in a compact 15mm x 15mm x 2mm package, with 2mm diameter, can be used. This aluminum coated mirror can address ±5° mech. angle (~20° FoV), with a bandwidth of ~1.5kHz. this 2mm MEMS mirror can still achieve a beam divergence of <0.1°, a typical specification in most LiDAR systems such as the Boeing Spectroscan3D (Figure 4b). The divergence of <0.1° can be maintained with using wide angle optics to expand the MEMS mirror's native FoV to larger ones such as 90° or greater (Figure 5a). The independent transmitter design also allows for a simplified transmit scan head design incorporating a compact MEMS mirror, diode laser or a fiber collimator as an input, and compact off-the-shelf lenses (Figure 5b). To compensate for the larger FoV of the transmitter, various designs have been presented, including partitioning off sections of the FoR into quadrants with independent receivers (Figure 5c) [18], to receiver arrays [19] with each pixel looking at smaller portions of the FoR.

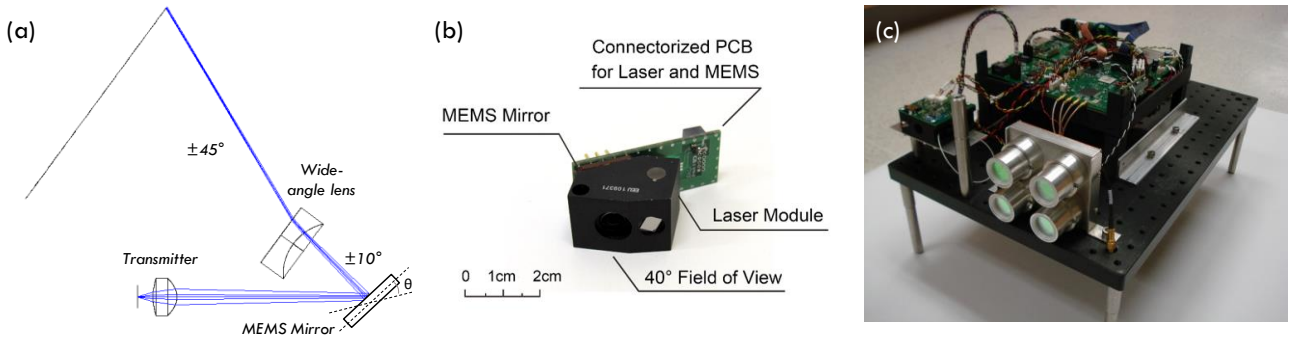

Figure 5. (a) An example of an optical train used to focus the transmitted beam onto the MEMS mirror and increase field-of-regard. (b) The EaZy 2.0 Scan Module (c) A bistatic LiDAR design from Army Research Labs (ARL) [18]

Commercialized products which implement this biaxial architecture, such as the aforementioned Boeing SpectroScan 3D, have been available on the market for several years [17]. The same biaxial setup based on the ARL reference design presented in [18] has also been adopted by other commercial (unpublished) LiDAR designs and by some published designs such as the Kodiak (formerly GRSSLI) LiDAR by the NASA GSFC team, slated for the Restore L missions [21]. Another very high performance LiDAR based on the biaxial architecture is from Beamagine, shown in Fig. 1 earlier.

2.3 MULTILAYER OR MULTIBEAM LIDAR

A third category, and one that is most used by various mechanical mirror scanning or spinning lidars (Figure 6c), uses multiple laser beams and a single axis scanner to achieve a 2D scan for 3D LiDAR [12][35] (Figure 6a). In this methodology, the vertical axis is generated by a movable prism or multiple transceivers and the horizontal axis is addressed using a single axis scanning mirror or a rotating servo spinning the vertical axis around [14]. A biaxial scanning mirror can also be used with multibeam LiDARs to expand the scanning mirror's native horizontal FoV. In the biaxial case, multiple transceivers are used at different angles of incidence to generate a larger FoV scan in the axis of incidence of the transceivers (Figure 6b). In the above-mentioned cases, the transceivers can be defined as the transmit laser and photodetector receiver in the coaxial or biaxial setups, where multiple laser sources and a single detector can be used in the case of the biaxial setup.

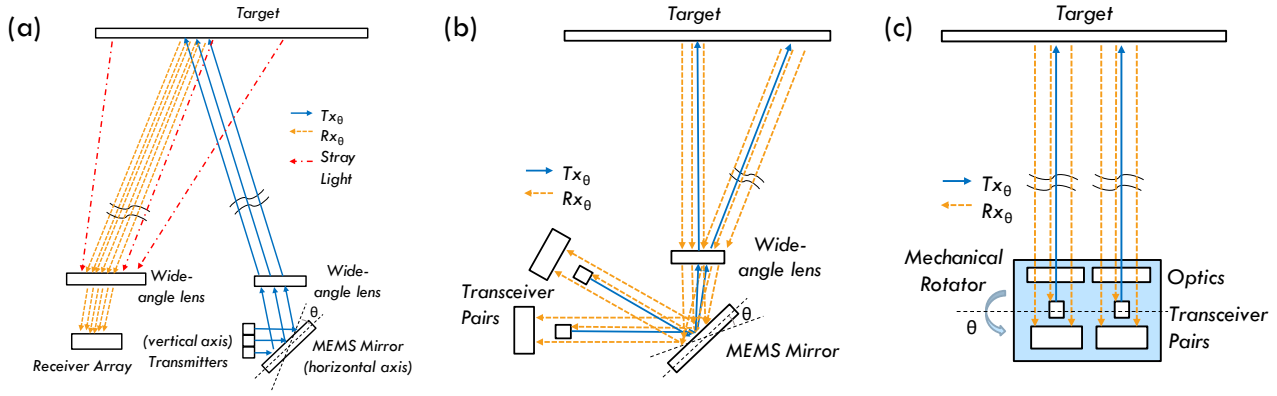

Figure 6. (a) A biaxial LiDAR design that utilizes transmitter and receiver arrays to increase measurements per second [40]. (b) A biaxial LiDAR design that incorporates two (or more) transceiver pairs in order to increase measurements per second. (c) An example of a spinning LiDAR design that places multiple transceiver pairs on a mechanical rotator to achieve a two- or three-dimensional point-cloud.

2.4 LASER AND EYE SAFETY CONSIDERATIONS

Note that we are only discussing here eye safety, rather than laser safety in general, as solutions with the potential for skin damage, material damage, and fire are beyond reasonable consideration for industrial and consumer products [32]. In fact, it is our opinion that the requirement for use of low power, material-safe and eye-safe is a leading requirement in the LiDAR design. The challenge for a successful design is then to achieve distance, angle, accuracy requirements while maintain Class I laser classification, i.e. classification as a product that is safe under practically all uses.

Eye safety is an important issue when it comes to laser-based product and MEMS Mirror based LiDAR products are in that category. The safety of eye depends on many factors such as wavelength of the laser used in the LiDAR, power of laser, duration of the pulse, divergence angle of laser beam typically defined by optics, and the exposure duration of the eye which determines the amount of the radiation energy received by an eye. There is a general understanding that visible laser light (400 nm to 700 nm) is harmful to an eye if the eye is exposed to damaging levels of radiation - therefore eye safety rules are defined to avoid potential injury to human eyes. These rules are governed by international standard IEC 60825-1 and CFR 1040.10 and 1040.11 via FDA in the USA. According to the rules, laser products are classified based on the amount of radiation that is deemed to be safe, and for the product to be classified in specific category it must not exceed the radiation energy defined for the given class. For example, Class 1 limits average power to <0.39mW to be safe under most circumstances. Class 2 defines products with the amount of unintentional radiation to eye retina that cannot exceed 1 mW for the period of 250 ms at the distance greater than 7 m from a source – but this category requires the beam to be visible in order to rely on eye's blink response for the added safety.

Today two types of infrared lasers are predominantly used in the LiDAR systems, 905 nm laser and 1550 nm laser, although a number of LiDAR systems can be found using visible green lasers and other wavelengths are considered too. However, use of visible light in automotive applications generally is not desirable since it can cause major distraction to other vehicles and traffic. The 905 nm wavelength is adopted initially for LiDARs because these pulsed laser diodes were readily available and relatively inexpensive and corresponding photosensors that are silicon-based were also mass produced and inexpensive. But safety consideration for this wavelength too had to be taken into account because eye

does transmit 905 nm light to retina, and therefore eye safety requires limiting laser power at this wavelength despite the fact that it is out of the visible spectrum. Because of the restriction in laser power with 905 nm wavelength these LiDARs are typically limited in range to about 100 m. To increase the range of LiDAR products designers have turned then to 1550 nm wavelength believing that 1550 nm is inherently safer since it is further away from visible light and the lasers can be cranked up with the higher power. This approach works, but it turns out that even 1550 nm wavelength could cause eye injuries [31], particularly cornea and lens can be damaged with the sufficient power, although the thresholds are higher than for retina at shorter wavelength. Bottom line, no matter what wavelength is used safety features are a must for LiDAR systems.

Since practical MEMS mirrors of practical speed, with adequate shock and vibration tolerance are relatively limited in diameter, it is typical that transmitted laser beam diameter is within the diameter of the fully dilated pupil (7mm) as called out in the laser classification guidelines. Thus, an eye safe MEMS-mirror based LiDAR system must output very low average optical power (<0.39mW) or adequately distribute (scan) the average power over a larger area and limit access to the output beam before the area is increased based on the FoV.

3. HYBRID APPROACH – SYNCHRONIZED MEMS PAIR LIDAR (SyMPL)

Given advantages and disadvantages of the two predominant MEMS Mirror LiDAR architectures – coaxial and biaxial – it is prudent to explore some combination of the two in an effort to maximize performance and simplify the design. The Synchronized MEMS Pair LiDAR (SyMPL) is a hybrid approach to MEMS Mirror LiDAR [22] designed to capitalize on the advantages of the biaxial and coaxial architectures while minimizing their disadvantages.

The SyMPL light imaging, detection and ranging system leverages our established MEMS mirror devices which are at the core of single-crystal silicon construction and are equipped with electrostatic comb-drive actuators on each end of a dynamic tilt axis. The exclusively electrostatic actuation has many benefits compared to piezo or galvanometer scanning technologies, namely robustness, repeatability, and very low power consumption (<1mW) while offering a virtually limitless lifetime as there are no elements on device level that degrade over time. Thus, a LiDAR built with these gimbal-less, electrostatic MEMS mirrors can be appropriately labeled as a solid-state LiDAR, limited only by the lifetime of its laser source. To solve the most challenging task of the LiDAR industry – mass production readiness at marketable cost – we designed an architecturally simple and low-cost arrangement of using own mass-produced MEMS Mirrors and off-the-shelf ToF laser ranging components. Fast, eye-safe laser range finders (LRFs) have become established in many formats and at low cost from many suppliers based on a number of reference designs offered to the designers. Optomechanically coupling them suitably with mirrors and driving the mirrors accurately results in extending their capability from 1D to 3D. With the addition of a compact and efficient Controller unit which provides an interface to software/APIs, the solution is complete and software-configurable.

Figure 7. (a) The SyMPL 3D LiDAR architecture uses two MEMS mirrors to direct the transmitted beam and the receiver's aperture simultaneously, to the same region. (b) An image of the scene addressed by the SyMPL 3D LiDAR. (c) The point cloud generated of the scene using SyMPL 3D LiDAR

The SyMPL architecture, as shown in Fig. 7a and Fig. 8b, uses two MEMS mirrors that are performing a synchronized scan together, with one mirror scanning the transmit beam, and one mirror directing the light back to the receiver. In this case, both the transmitter and receiver are pointing at the same angle, and neither the transmitter or receiver are obstructed by each other or other beam splitting optics which was the challenge of coaxial designs. The transceiver assembly in this

case would be simplified, where only the transmitter or receiver needs to optically be aligned to each individual MEMS mirror, and the two MEMS mirrors can be aligned together to address the same angle within the overall FoV. This design also allows for flexibility in the MEMS mirror selection, where the mirror diameter and angle can be traded towards increasing bandwidth (e.g. smaller diameter mirror) or increasing the ToF range distance (e.g. with a larger diameter mirror while keeping laser power very low). The MEMS can be calibrated or trained to ensure the desired angular resolution is reached, and the FoV requirements are met. Additional sensors can also be integrated into the transmitter side MEMS mirror to monitor the position of the mirror for laser-safety considerations (interlocking with the laser driver), and if necessary to place the MEMS mirror under closed-loop control. We present more on the section of MEMS Mirrors for SyMPL in Section 4.1, and the driving methodologies in Section 5.

This architecture is particularly simple, as seen in Fig. 8b, as it only requires a typical single-point LiDAR (or LRF) to be pointed at two MEMS mirrors which are spaced accordingly. But we note that the simplicity of achieving high performance with such an arrangement is mostly owed to the extreme repeatable accuracy of the electrostatic gimbal-less MEMS mirrors utilized in the pair. The synchronized MEMS pair aspect of this design could easily be a major technical challenge and significant undertaking with the need for complex control systems and synchronization algorithms and schemes, were it not for the specific gimbal-less MEMS mirrors with dual-axis quasistatic actuation.

Initial prototyping of the SyMPL (Figure 7) was done using an OEM laser rangefinder (LRF) sensor, similar to the work presented in [23]. There are many such off-the-shelf LRFs available for use as "single-point LiDARs" for many applications. Typically, there is a transmitter output lens and a receiver input lens next to it, and both are designed to have a very narrow iFOV, addressing a small point in the distance and reporting its distance. If each of those optical axes is then matched with a MEMS mirror which deflects it in a desired direction, and if both mirrors can be aimed synchronously, we can quickly turn the single-point LiDAR into a 3D LiDAR (Figure 8b). The OEM versions of the LRF ToF sensors have a UART interface that allows for flexibility in how the sensor is used – and additionally allows the distance information to be acquired by the MEMS Controller. The sample rate, minimum and maximum range information and other variables were available for the user for adjustment and easy to evaluate. This module allowed us to put together prototypes to evaluate various MEMS mirrors presented in the Hardware MEMS mirrors section.

Further optimization of the initial design followed by using custom ToF sensor hardware, allowing for direct access into the pulse train generation and receiver electronics to increase sample rates, develop custom interface protocols and provide a user socket to interface with 3rd party systems. The various hardware components in the ToF that were evaluated are presented in the Hardware Time of Flight (ToF) Setup section 4.4 below.

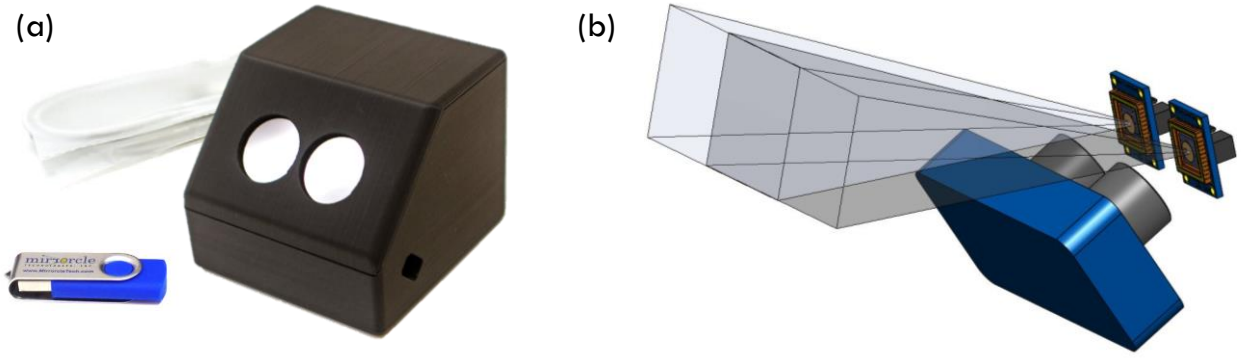

Figure 8. (a) The first commercially available version of the SyMPL 3D LiDAR. (b) A three-dimensional diagram of the SyMPL showing the two MEMS mirrors, time-of-flight module in blue, the optics in gray, and the overlapping FoV of the two MEMS mirrors. As the distance increases, FoV of the two MEMS mirrors will overlap completely.

4. HARDWARE AND SOFTWARE SETUP

4.1 SELECTION OF MEMS MIRRORS

Many different MEMS mirror devices from our product portfolio have been evaluated for coaxial, biaxial and the SyMPL hybrid scanned LiDAR architectures. Four most notable designs have been chosen for a more detailed study, as detailed shown in Figure 9. All four MEMS mirrors are designed for two-axis quasistatic (point-to-point) beam steering. Many

other designs and products including single-axis mirrors like A8L2.2-2400x6000AL (2.4mm x 6.0mm rectangular mirror) were evaluated by universities, research and commercial organizations developing their own LiDARs, but are not reported here. The devices studied herein were selected based on their scan angle capabilities, mirror diameters, and device bandwidths, key parameters to determine potential use in specific applications. For example, the 2.0mm mirror fits the needs most biaxial cases, has been demonstrated to pass various shock and lifetime tests as well as laser power handling in lighting applications [25]. Coaxial LiDAR applications typically require a large diameter mirror to scan the laser over the FoR and receive enough reflected light back for accurate time of flight (ToF) measurements. In initial coaxial tests, the largest diameter mirrors such as the A5L3.3-6400AU was used to maximize the transceiver aperture but was not large enough to measure the distances required in mid-range LiDARs (30m). For the SyMPL hybrid approach, the A7B1 actuator was chosen for the larger optical FoV at 32° with a 3mm diameter mirror, and the A8L2.2 actuator was chosen to evaluate a larger diameter mirror with 4.6mm diameter. All four mirrors have their own benefits and limitations, with the key feature highlighted in the bottom row in the table in figure 9.

4.2 MEMS DRIVERS

The gimbal-less MEMS mirrors with bi-directional electrostatic rotators [30] have a unique Biased Differential Quad (BDQ) channel driving scheme, and are driven using compact and low-power consuming high voltage MEMS drivers [33]. There are various levels of integration when it comes to MEMS drivers, starting from a basic driver with analog voltage or digital SPI signal inputs. These drivers can be incorporated into higher level controller designs, but in typical LiDAR applications, the processing and control of the MEMS mirror may be done on complex microcontrollers or FPGA, and therefore may require bespoke electronic design based on the user's requirement.

	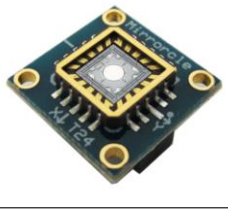	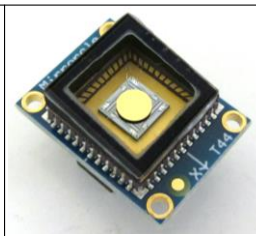	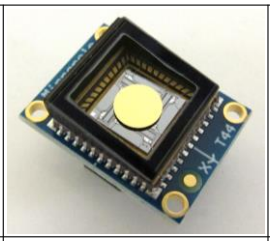	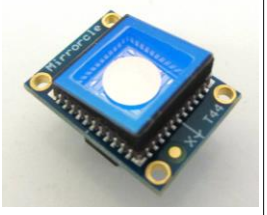
MEMS Mirror	A7M20.2-2000AL	A7B1.1-3000AU	A8L2.2-4600AU	A5L3.3(C1)-6400AU
Package and Cover	TINY20.4-NW	TINY48.4-B/W/TP	TINY48.4-B/W/TP	TINY48.4-B/W/TP
Mirror Diameter	2.0mm	3.0mm	5.0mm	6.4mm
Optical Angle	±10°	±16°	±11°	±5°
First Resonance	1300Hz	400Hz	350Hz	300Hz
Feature	highest bandwidth	largest angle	largest theta-diameter	largest mirror diameter

Figure 9. A table of MEMS mirror choices that were investigated and recommended for most LiDAR applications.

These MEMS drivers (Figure 10b) are designed to be compact, consuming less than 100mW of power and small enough to be integrated into most electronic designs. The critical components of the driver are the low voltage signal processing section such as the 4-channel DAC (or op-amps in analog-input version) to generate the 2 differential pair drive signals, a DC/DC block to generate the high voltage supply, and a 4-channel high voltage op-amp. Additional components such as filters can be used to smooth out the low voltage signals to limit the bandwidth of the MEMS mirror and prevent from exciting resonant frequencies. The driver has a large signal bandwidth of >25kHz which is adequate for any driving methodology. The bandwidth is limited only by the high voltage amplifier, however in typical applications it is limited at a lower value by the on-board filters with cut-off frequency that can be adjusted based on the device's parameters.

4.3 CONTROLLERS

For applications like this Hybrid LiDAR system SyMPL that require a higher level of integration, MEMS Controllers nicknamed "OCCIE" have an embedded MEMS driver similar to the ones described in the driver section (2.3), along with a microcontroller (Microchip part PIC32MZ) to provide higher level functions. The MCU enables the user to communicate with the software level to exchange information with the ToF block as well as control the MEMS mirror by downloading and running custom content, etc. These Controller boards are based on the larger USB-SL MEMS Controllers, customarily ship with the company's plug-and-play development kits. Both the OCCIE and USB-SL MZ controllers are USB-powered and –controlled and offer ready-to-use control electronics to allow for instant experimentation with MEMS mirrors using Windows applications [33]. The controllers also have APIs available on

several different development platforms – namely C++, LabView, MATLAB and Python SDKs as well as Java (Android) SDK.

The established OCCIE Controller is pictured in Figure 10c. The controller weighs ~100g and comes in a compact 70mm x 40mm x 15mm. Along with the MEMS driving capabilities, the controller also has two analog inputs, 8 channels of correlated digital outputs to trigger additional controllers or driving of lasers, cameras or other peripherals, a synchronization port that can either send or receive external triggers or clocks, and a host connector port to interface with other development boards used by Mirrorcle internally. In the case of SyMPL, the ToF digital circuit and power supply is in the development board, connected via the digital and host connector headers. This flexibility in the design allows for rapid prototyping and development of various technology platforms like the RGB Playzer or 3D Scanning and Metrology on the same OCCIE controller platform.

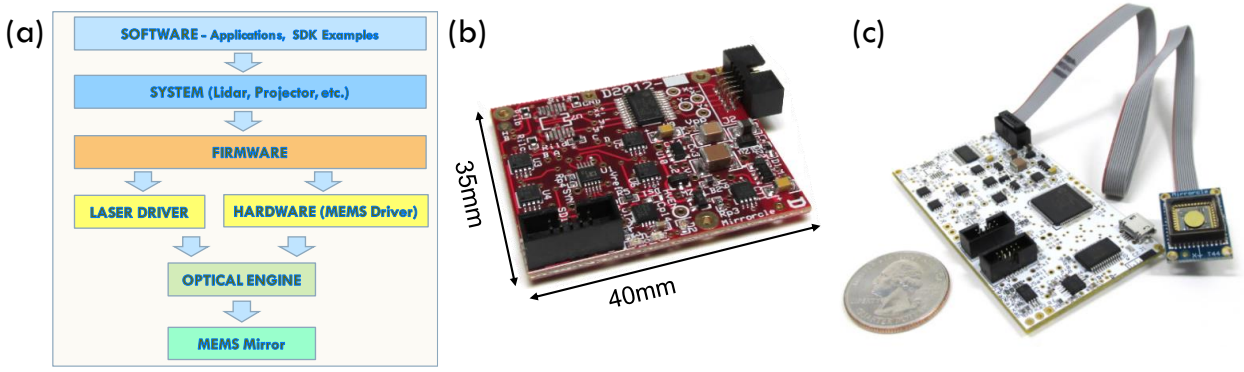

Figure 10. MEMS Mirror control and driving overview: (a) Layers of integration from software layer with user/system command of mirror movement all the way down to the MEMS Driver electronics and finally the mirror itself. (b) MEMS driver – SPI based digital input for driving of electrostatic gimbal-less dual-axes MEMS mirrors, (c) The OCCIE MEMS controller with an integrated MEMS driver, a PIC32MZ processor, USB power and interface.

4.4 TIME OF FLIGHT (TOF) SETUP

To move beyond the limitations of off-the-shelf LRFs which typically have limited data rates, we evaluated various ToF designs both for the transmitter and receiver components individually. The critical component in the ToF setup was the receiver electronics being able to detect nanosecond pulses. Here designs using high bandwidth Analog to Digital Converters (ADCs) and Time to Digital Converters (TDCs) were investigated, both widely used and recommended in reference designs by the major mixed-signal chip manufacturers. As for the transmitter design, the simplest approach was using the low-cost and widely available SPL PL90 905nm pulsed laser diode from OSRAM [26]. Using a 905nm laser also enabled the use of low-cost Silicon based photo-detectors. OSRAM recommends pairing the SPL PL90 with the SHA2400 Silicon PIN photosensor [26]. The PIN photosensor design is a simpler design, requiring a low voltage supply (12V) to bias the photodiode. An alternate approach to the PIN photosensor is the Avalanche Photodiode (APD). APDs are more sensitive to nanosecond pulses but require a high voltage supply to act as a bias to minimize the photodiode's capacitance and maximize the diode response time [28][29].

The transmitter side required the generation of very short nanosecond pulses to driver the pulsed laser. The 75W pulse SPL PL90 laser diode requires forward voltages of 6-10V, with peak forward currents of 40A. High-speed and high-power handling components were required for the laser driver and a reference from EPC Co. [27] was used to generate the pulsed driver with an adjustable pulse width. The reference circuit uses two different low pass filters to generate a short delay between two copies of the start trigger, and AND-gated together to create a short pulse. The pulse width is controlled by adjusting the filter cut-off of the low pass filters.

4.5 SOFTWARE AND FIRMWARE

Throughout the development and testing of various LiDAR systems, including the SyMPL 3D LiDAR, the firmware and software were built using the Mirrorcle application programming interface (API). This significantly decreased initial engineering time and reduced system complexity as the foundation of both the firmware and hardware was well-established with multiple years of production status. Furthermore, the API enables software development kits (SDKs) in multiple programming languages, including C++, Matlab, LabView, Python, and Java. Flexibility across languages facilitated quick experimentation and development in Matlab and Python while later allowing performance-oriented applications to be developed in C++.

Within the API, the firmware is built on Microchip's PIC32MZ MCU. The firmware allows for communication over USB to a host PC. The host PC forwards commands, streams of positional coordinates, and various data/position transformations to the firmware, which then outputs the final MEMS positions to a 16-bit DAC. Range measurement are returned to the firmware via analog or digital interface and provided to the host PC as a stream of Z data.

Two software applications were created to allow communication and control with the LiDAR systems. The first, MirrorcleLiDAR, is a Windows-based C++ application that generates scan patterns for the LiDAR and handles the flow of data between the host PC and the LiDAR. MirrorcleLiDAR allows users to set scan parameters such as scan size, speed rotation, and position/offset as well as the number of lines and how control waveforms and returned data are filtered. Additionally, MirrorcleLiDAR draws a polar plot of a cross-section of the data, enabling immediate feedback from the LiDAR (Figure 11b). The second software application, MirrorcleCloud, is a C# (Unity Engine) application built to visualize three-dimensional point clouds. MirrorcleCloud has features to enable control of viewing angles, position, field of view, and zoom to clearly visualize and navigate a point cloud (Figure 11c).

These two applications communicate via a server-client architecture, utilizing the TCP/IP communication protocol to exchange the LiDAR point cloud data over a UDP socket. A proprietary protocol was developed to efficiently provide the final X, Y, Z data to UDP clients that is resilient to interruptions or dropped packets. Figure 11a shows a diagram of the server-client architecture used by MirrorcleLiDAR to serve point cloud data as the middle-man between the SyMPL 3D LiDAR and client applications that receive the data, such as MirrorcleCloud. This architecture is constructed such that any computer vision or visualization application can receive data as the client when listening to the MirrorcleLiDAR UDP server. Together, the firmware and software in the API were built with the focus on programmability. The emphasis of a MEMS Mirror LiDAR system is customizable scan patterns, and the software applications were constructed to enable this unique capability.

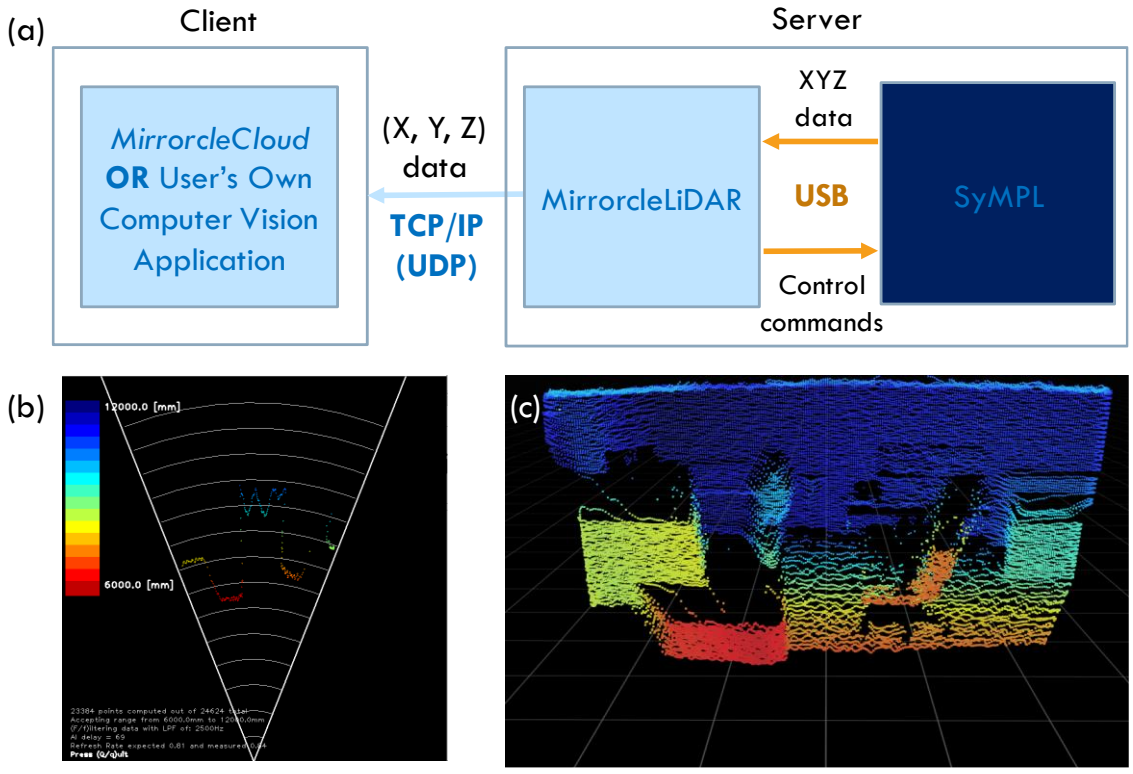

Figure 11. Mirrorcle LiDAR software: (a) Diagram of the server-client architecture employed by SyMPL 3D LiDAR and supporting software to process and serve point cloud data to client applications (b) a top down RADAR cross-section view of the FoR being scanned by the SyMPL, (c) a 3D point cloud from the same FoR from (b) of various objects 10-15m away.

It should be stressed that the SyMPL 3D LiDAR system is supported by an intuitive software package that enables programmable control of the LIDAR as well as detailed point cloud visualization – with SDKs for multiple computing platforms. Users will be able to immediately see and interact with a real-time, three-dimensional point cloud from the SyMPL, "straight out of the box." The software package will allow the user to go beyond viewing the point cloud. Users

can quickly begin incorporating the SyMPL solution into their own systems by interfacing with the easy-to-use server-client system. Extensive documentation and a lightweight communication protocol are critical to enabling integration of a LiDAR sensor into a guidance or mapping system. Ease of integration into existing systems is the core paradigm around which the software was built.

5. CONTROL OF MEMS MIRRORS

5.1 OPEN LOOP

Extremely high repeatable accuracy of laser beam steering in this technology is inherent in the construction of the MEMS mirror itself. Namely, owing to their pure Single-Crystal-Silicon construction, and electrostatic driving, these MEMS mirrors are frequently employed in real world imaging and metrology applications with open-loop (feed forward) driving due to the high repeatability of the static and dynamic responses. Typical specifications are a resolution of 10k x 10k (x-axis x y-axis) easily (with relatively simple circuits) repeatable positions. This means that in a ±10° optical scanning angle , we can programmatically set the direction of the beam repeatably within 2 milli-degrees. Silicon and electrostatic driving methodology additionally has a small temperature sensitivity so the overall characteristic is very high precision in a wide range of environmental settings which is easily translated into very high accuracy by way of calibration (for example obtaining a LUT).

The Mirrorcle MEMS mirror technology stack (Figure 10a) starts at the core of MEMS mirror at the bottom of the stack and builds upon driver and controller hardware with a firmware interface to the top with software and applications layer. The software API layer is available on variety of different development platforms to drive the MEMS mirror via the MEMS controller, help generate waveforms, and transform and filter the waveforms. The software layer enables rapid development of the LiDAR platform, enabling the user to try different waveforms, sample rates, line times, frame rates, resolution and angles. In the case of the SyMPL LiDAR, there are a few different methodologies on the type of waveform scanned over the FoV to image as much detail as possible. The API layer has functions in the MTIDataGenerator class to create specific waveforms such as a linear raster pattern, where the horizontal axis is uniform velocity lines or triangle waves, and the vertical axis is a slow sawtooth waveform that increments for each line in the frame. Another type of waveform used is the Resonant Quasistatic (RQ) raster pattern. In the RQ case, the horizontal axis is being scanned with a sinusoid waveform, typically at frequencies close to the device's resonance to minimize the line time, to improve the frame rate of the scan. The third, broader, category is an arbitrary waveform – which can be a mix of sinusoidal waveforms to create a Lissajous pattern, or any other waveform that directs the MEMS mirror to scan or address very specific pixels anywhere within the FoV. All this customization is available alongside the MTIDevice class of functions which lets the user set various amplitude, sample rate, filter settings to improve the MEMS mirror's performance. In all these above cases, the MEMS mirror is being driven in open loop – meaning that the MEMS mirror is performing the scan as prescribed via the software, and not taking into consideration some of the non-linear affects that may take place at large angles or frequencies close to the device's resonant frequency. These non-linearities are reduced by filtering the waveform and avoiding any frequencies that excite the device's resonance. In the case of non-linear voltage vs. angle response, a look-up-table (LUT) can be applied to linearize the device's response.

There are methods to help improve the linearity and the bandwidth of the device, such as applying an inverse filter as presented in [30], while still running in open loop, or training the device by observing the device's behavior and correcting any non-linearities using a control loop. We present two different approaches to training a MEMS mirror in the next sections below.

5.2 TRAINING WITH ILC

As previously discussed in detail [30], in applications where the MEMS mirror performs a scan that is known *a priori*, such as a linear raster pattern or an RQ raster pattern, the waveform can be speed- and linearity-optimized by training the waveform based on an optical sensor for feedback. Over a number of converging iterations, based on the sensor data of beam steering position over time, the ILC training system can improve the driving waveform to remove any of the non-linear effects of the device, and achieve the scan as prescribed. This methodology is called Iterative Learning Control (ILC). In the setup we utilize a simple laser test beam (lower power CW laser) and aim the scanned beam onto a duo-lateral PSD. The resulting scan is then sent back to the host via ADCs from the MEMS controller and is compared against the setpoint waveform. The error is calculated, and a correction waveform is generated as a result to be sent to the MEMS mirror again. This process is repeated until the error is reduced to a metric defined by the user. For example, in most LiDAR applications, x-y accuracy of <0.1° is typically required, so a trained waveform with a scanning error within 0.01° can be used which is easily attained by this methodology [30]. One major advantage of this approach to waveform

optimization, leading to higher tracking accuracy is that the iterative process with run to run adjustment allows acausal treatment of waveforms – determination of adjustment at each sample can utilize knowledge of past and future samples – this is impossible in real-time (e.g. PID) control loops.

5.3 CLOSED LOOP CONTROL

Although precision of the electrostatic MEMS mirrors is often highest in open loop/feed-forward driving, closed loop control may also be employed due to its advantages. Firstly, a separate test beam is used in the LiDAR's optical system regardless of the driving methodology in most implementations, and that is due to the need to monitor the responsiveness of the MEMS mirror to ensure system's eye safety and meeting of the laser classification. Namely, classification as Class 1 device based on low average power of the laser *and* the fact that the beam is continuously scanned requires that the scan is reliably monitored.

With the position of the scanned beam monitored for eye safety purposes, if the sensor has good enough data (low noise, fast sample rate), it may additionally be used for closed-loop control. An optical position sensor observes the MEMS mirror position in real time, and the position data is sent back to the controller level to process and correct for any error between the setpoint and the final output of the waveform. This requires additional hardware within the optomechanical setup for the position sensor, and additional computational power at the controller level to process the error in real time. However the additional hardware and computation power may already be integrated as mentioned for compliance with various certifications.

6. TECHNOLOGY ROBUSTNESS

The Single-Crystal-Silicon also has other properties that make the MEMS mirror a robust and reliable technology that can be used in consumer, automotive and industrial technologies. We have presented the results of mechanical shock and vibration, lifetime tests, temperature tests and laser power handling in previous papers [30][34]. In the sections below, a brief summary is provided on the robustness of the devices specifically for LiDAR.

6.1 MECHANICAL SHOCK

The integrated MEMS mirror devices such as the A7M20.2-2000AL and the A5M24.3-2400AL that can be used in biaxial LiDAR configurations have a high tolerance for mechanical shock and vibration. Testing has shown that these integrated devices can pass the mechanical shock tests outlined in MIL-STD-883 Method 2002, Condition A, shocking all six axes with 1ms of 500G peak shocks [24]. The larger bonded mirror designs such as the A8L2.2-4600AU and A5L3.3-6400AU have had their predecessor designs tested for shock, surviving 300G peak shocks with 1ms impulses. Based on those previous shock test results, the current generation of the bonded devices have additional design considerations to be more robust to shock and vibration. All of these MEMS mirror devices, both integrated and bonded mirror design types, can qualify the 20G vibration tests from 20Hz to 2000Hz, as outlined in MIL-STD-883 Method 2007, Condition A [24].

6.2 LIFETIME TESTS

As of 2019, Mirrorcle has performed numerous in-house lifetime tests, of both MEMS mirrors and MEMS drivers. In most cases, the test conditions were at room temperature, with standard operating voltages. In some specific cases, driven by customer requirements, devices were tested at elevated temperatures and voltages. In all these test conditions, the MEMS mirrors were able to complete billions of cycles (2500+ hours), without any mechanical related failures. One key failure that was identified from root-cause analysis has led to improvement in the epoxy used to die bond the MEMS devices into the package, and further tests have showed no failure due to epoxy.

In addition to the MEMS devices, MEMS drivers and controllers were tested alongside the EaZy 2.0 scan modules (Figure 5b), for billions of cycles, checking the lifetime of the electronic components, the laser used in the scan head, and the core component of MEMS mirror. After 4000+ hours of testing, all the scan modules and controllers were functioning properly, without any issues.

6.3 OPERATION TEMPERATURE

All Mirrorcle MEMS mirrors are rated to operate from -40°C to +105°C. The operating temperature range makes the MEMS mirror a viable component in most industrial and automotive applications. Beyond the MEMS mirror, the current design of the MEMS driver and controller have components rated for from -40°C to +85°C, and on a path towards replacing critical ICs with automotive qualified ones. The purely Single-Crystal Silicon construction of the device make it very repeatable over the operating temperature range, where a LUT can be applied to model the MEMS mirror behavior

at different temperatures. In-house elevated temperature testing has shown that the laser diode and other electronic components may fail before the MEMS mirrors.

6.4 MIRROR REFLECTIVITY AND POWER HANDLING

Mirrorcle MEMS mirrors come with two standard optical coatings of Aluminum (Al) and Gold (Au). With the standard Al coating and additional heatsink structures in the ceramic packaging to help dissipate heat from the MEMS mirror, Mirrorcle has demonstrated laser power handling of up to 8W of CW power at 450nm wavelength [34]. In the case of 1550nm, the same Al coated mirror has been used in numerous LiDAR applications [18][21], demonstrating the capability of the mirror to handle the high energy pulses needed for scanned LiDAR applications.

In the case of NIR wavelengths, e.g. 905nm, the Au mirror coating is recommended since the Al has a drop-off in reflectivity around 800nm to 1000nm. The Au coating has also demonstrated capability of handling the pulsed laser powers of the SPL PL90 laser diode, and the MEMS mirrors used in the SyMPL prototypes all have the Au coating.

7. CONCLUSIONS

When it comes to perception sensing, LiDAR technology has found itself in the limelight in the past decade because of the clear advantages it offers when compared to other technologies such as RADAR, cameras and ultrasound sensing. Comparative analysis in performance shows LiDAR's advantage in several areas including low average power, distance resolution in sub-cm range, superior object detection of varied materials and reflectance, and fast scanning with programmable capability. When these advantages are combined with the potential of a significant cost reduction it becomes clear why LiDAR technology is considered to be a major contender for many applications such as robotics, automotive safety features including autonomous driving, drones, many industrial and commercial applications, as well as aerospace and medical applications.

LiDAR technology has several variances ranging from mechanical spinning of prisms, to optical phase array, to MEMS-mirror based solutions. One should notice a general trend of moving away from bulky mechanical and motor-based systems towards compact silicon-based MEMS technology. Thus, in this paper we focus exclusively on MEMS-mirror based solutions. We have analyzed two major architectures – coaxial and biaxial. In coaxial architecture LiDAR scans the outgoing laser beam and receives the reflected light back to the receiving sensor using the same MEMS mirror, while in biaxial architecture LiDAR places the receiving sensor in an offset position from the transmitter and scanning components. The advantage of the coaxial architecture is that there is no interference between transmit and receive path but in general it requires larger MEMS mirror which leads to reduction in speed and robustness. On the other hand the advantage of biaxial architecture arrives from the fac that it can employ smaller high-bandwidth MEMS mirrors that leads to increased scanning speeds; also smaller mirrors have a higher natural resonant frequency which makes them more robust to shock and vibration.

We have also presented in this paper a hybrid architecture, a combination of the two in an effort to maximize performance and simplify the design. The Synchronized MEMS Pair LiDAR (SyMPL) is a hybrid approach to MEMS Mirror LiDAR architecture designed to capitalize on the advantages of the biaxial and coaxial architectures while minimizing their disadvantages. Mirrorcle's team has designed an architecturally simple and low-cost arrangement of using own mass-produced MEMS Mirrors and off-the-shelf ToF laser ranging components. Namely, fast eye-safe laser range finders (LRFs) have become readily available and coupling them optomechanically with mirrors and dedicated mirror drivers can lead to extending LRFs capability to 3D. With the addition of a compact and efficient controller unit which provides an interface to software/APIs, the solution is complete and software-configurable.

8. REFERENCES

[1] Guttman, U., Papst, J., Merlo, R., Kane, D., Bieser, G., and Grob, O., "Industry 4.0: What's Next," SAP White Paper, SAP SE, May 2017. Web. Dec. 2019. https://www.sap.com/documents/2017/05/bae613d3-b97c-0010-82c7-eda71af511fa.html.

[2] "The Autonomous Industrial Revolution," Technical Articles, Analog Devices. Web. Dec. 2019. https://www.analog.com/en/technical-articles/autonomous-industrial-revolution.html.

[3] Choi, S., Thalmayr, F., Wee, D., and Weig, F., "Advanced driver-assistance systems: Challenges and opportunities ahead," Semiconductors, McKinsy and Company. Feb. 2016. Web. Dec. 2019

https://www.mckinsey.com/industries/semiconductors/our-insights/advanced-driver-assistance-systems-challenges-and-opportunities-ahead.

[4] Shaheen, S., Totte, H., and Stocker, A., "Future of Mobility White Paper," UC Berkeley: Institute of Transportation Studies at UC Berkeley, 2018; doi:10.7922/G2WH2N5D.

[5] Estl, H., "Paving the way to self-driving cars with Advanced Driving Assistance Systems," Texas Instruments, Aug. 2015. http://www.ti.com/lit/wp/sszy019/sszy019.pdf.

[6] Sagar, R, "Making Cars Safer Through Technology Innovation," Texas Instruments, Jun. 2017. http://www.ti.com/lit/wp/sszy009a/sszy009a.pdf.

[7] Jacobs, C., "Driver Assistance to Driver Replacement: The Cognitive Vehicle Is Built Upon Foundational, High Integrity Sensor Data," Technical Articles, Analog Devices, Web. Dec. 2019. https://www.analog.com/en/technical-articles/driver-assistance-to-driver-replacement.html

[8] Tummala, R. R., "Autonomous Cars: Radar, Lidar, Stereo Cameras," IEEE-CPMT Workshop – Autonomous Cars, Georgia Institute of Technology. 2017. http://ewh.ieee.org/soc/cpmt/presentations/cpmt1703f.pdf.

[9] Sekel, N. and Singh, A., "Physics of 3D Ultrasonic Sensors," Research Gate, Jul. 2019; doi: 10.13140/RG.2.2.25396.19849.

[10] "Ultrasonic Sensors Knowledge (Part 2): Influences on the Sound Beam," What's New?, Pepperl and Fuchs, Apr. 2014. Web. Dec. 2019. https://www.pepperl-fuchs.com/usa/en/25425.htm

[11] Adams, M. D., "Coaxial range measurement – current trends for mobile robotic applications," IEEE Sensors Journal, 2(1), 2-13 (2002); doi: 10.1109/7361.987055.

[12] Xu, F., Qiao, D., Song, X., Zheng, W., He, Y., and Fan, Q., "A Semi-coaxial MEMS-based LiDAR," IECON 2019 - 45th Annual Conference of the IEEE Industrial Electronics Society, 6726-6731 (2019); doi: 10.1109/IECON.2019.8927392.

[13] Richter, S., Stutz, M., Gratzke, A., Schleitzer, Y., Krampert, G., Hoeller, F., Wolf, U., Riedel, L., and Doering, D., "Position sensing and tracking with quasistatic MEMS mirrors," Proc. SPIE 8616, 86160D (2013); doi: 10.1117/12.2009439

[14] Hall. D. S., "High definition lidar system," United States Patent US 7,969,558. United States Patent and Trademark Office. Jun. 2011.

[15] Kim, G. and Park, Y., "Independent Biaxial Scanning Light Detection and Ranging System Based on Coded Laser Pulses without Idle Listening Time," Sensors, 18(9), 2943(2018); doi: 10.3390/s18092943

[16] Eom, J., Kim, G., Park, Y., "Mutual interference potential and impact of scanning lidar according to the relevant vehicle applications", Proc. SPIE 11005, Laser Radar Technology and Applications XXIV, 110050I (2 May 2019); https://doi.org/10.1117/12.2518643

[17] "Spectrolab 3D MEMS LIDAR System Model MLS 21," Spectrolab Inc., Nov. 2012. Web. Dec. 2019. http://www.spectrolab.com/sensors/pdfs/products/SPECTROSCAN3D_RevA%20071912.pdf.

[18] Stann, B. L., Dammann, J. F., and Giza, M. M., "Progress on MEMS-scanned ladar," Proc. SPIE 9832, 98320L (2016); doi: 10.1117/12.2223728.

[19] Hata, T., Ozaki, N., Murakami, Y., Azuma, K., Shinji, K., and Yanai, K., "High Resolution LiDAR Based on Single Chip SPAD Array," SAE Technical Paper 2019-01-0119, 9(2019); doi: 10.4271/2019-01-0119.

[20] Koppal, S. J., Tasneem, Z., Wang, D., Xie, H., "Directionally Controlled Time-of-Flight Ranging for Mobile Sensing Platforms," Robotics: Science and Systems, (2019)

[21] Petrick, D., Gill, N., Hassouneh, M., Stone, R., Winternitz, L., Thomas, L., Davis, M., Sparacino, P., and Flatley, T., "Adapting the SpaceCube v2.0 Data Processing System for Mission-Unique Application Requirements," Adaptive Hardware and Systems (AHS) 2015 NASA/ESA Conference, IEEE, 1-8 (2015).

[22] "Mirrorcle targets robotics with MEMS lidar," optics.org, Nov. 2019, Web. Dec. 2019. https://optics.org/news/10/11/34

[23] Kasturi, A., Milanović, V., Atwood, B.H., Yang, J., "UAV-Borne LiDAR with MEMS Mirror Based Scanning Capability," SPIE Defense and Commercial Sensing Conference 2016, Baltimore, MD, April 20th, 2016.

[24] MIL-STD-883E, "Test Method Standard – Microcircuits," 31 December, 1996. Dept. of Defense.

[25] Kasturi, A., Milanović, V., and Yang, J., "MEMS Mirror Based Dynamic Solid State Lighting Module," Journal of the Society for Information Display, Display Week 2016, May 2016.

[26] OSRAM-OS. "SPL PL90_3 Datasheet." Datasheet, Version 1.5, 2018-07-11.

[27] EPC-Co. "Development Board EPC9126 Quick Start Guide." Development Guide, Version 2.5, 2018.

[28] Texas Instruments. "TDC7201-ZAX-EVM User's Guide." SNAU198A–May 2016–Revised May 2016

[29] Texas Instruments. "Time-of-Flight Camera – An Introduction." Technical White Paper, SLOA190B – January 2014. Revised May 2014.

[30] Milanović, V., Kasturi, A., Yang, J., Hu, F., "Iterative Learning Control Algorithm for Greatly Increased Bandwidth and Linearity of MEMS Mirrors in LiDAR and Related Imaging Applications," SPIE 2018 OPTO Conference, San Francisco, CA, Feb. 2018

[31] Schulmeister, K., "The new edition of the international laser product safety standard IEC 60825-1," SEIBERSDORF LABOR GMBH 2017.

[32] Lee, T.B., "Man says CES lidar's laser was so powerful it wrecked his $1,998 camera." Ars Technica, Jan 11 2019. https://arstechnica.com/cars/2019/01/man-says-ces-lidars-laser-was-so-powerful-it-wrecked-his-1998-camera/

[33] "PDF Guides and Resources," Mirrorcle Technologies, Inc., Web. Jan. 2020. https://www.mirrorcletech.com/documentation/Guides/PDF%20Resources.html

[34] Kasturi, A., Milanović, Veljko., Hu, F., Kim, H., Ho, D., Lovell, D., "MEMS mirror module for programmable light system." SPIE Photonics West 2019, MOEMS and Miniaturized Systems XVIII, San Francisco, CA. Feb 2019.

[35] Druml, N., Maksymova, I., Thurner, T., Lierop, D.V., Hennecke, M., Foroutan, A., "1D MEMS Micro-Scanning LiDAR," The Ninth International Conference on Sensor Device Technologies and Applications, SENSORDEVICES 2018.

[36] Hofmann, U., Senger, F., Soerensen, F., Stenchly V., Jensen, B., Janes, J., "Biaxial Resonant 7mm-MEMS Mirror for Automotive LiDAR Application," IEEE 2012.

[37] Hasselbach, J., Kastner, F., has, R., Bogatscher, S., Rembe, C., "Demonstration of a MEMS Mirror, 3D-LiDAR System with Large Aperture and Scanning Angle," IEEE 2019.

[38] Tanahashi, Y., Koutsuka, Y., Tanimoto, R., Kawabata, C., Noda, S., et al. "Development of coaxial 3D-LiDAR systems using MEMS scanners for automotive applications," Proc. SPIE 10757, Optical Data Storage 2018: Industrial Optical Devices and Systems, 107570E (14 September 2018); doi: 10.1117/12.2323693.

[39] Lee, J. S., Lim, J., Moon, S., Lee, J., Kim, K., Park, Y., Lee, J.H., "MEMS Scanner-Based Biaxial LiDAR System for Direct Detection of Three-Dimensional Images," International Conference on Optical MEMS and Nanophotonics, 2018.

[40] Ito, K., Niclass, C., Soga, M., Matsubara, H., Aoyagi, I., Kato, S., Kagami, M., "Design and characterization of a 256x64-pixel single-photon imager in CMOS for a MEMS based laser scanning time-of-flight sensor." 21 May 2012 / Vol. 20, No. 11, OPTICS EXPRESS 11863, Optical Society of America, 2012.